
APPLICATION OF DEEP NEURAL NETWORKS TO LEARN SPECIES CONSERVATION EQUATIONS

Amol Salunkhe

Department of Computational Data
Science and Engineering
University at Buffalo
Buffalo, NY 14260
aas22@buffalo.edu

Siddhant S. Aphale

Department of Mechanical and
Aerospace Engineering
University at Buffalo
Buffalo, NY 14260
saphale@buffalo.edu

Vedant T. Joshi

Department of Mechanical and
Aerospace Engineering
University at Buffalo
Buffalo, NY 14260
vedantt@buffalo.edu

Varun Chandola

Department of Computational Data
Science and Engineering
University at Buffalo
Buffalo, NY 14260
chandola@buffalo.edu

Paul Desjardin

Department of Mechanical and
Aerospace Engineering
University at Buffalo
Buffalo, NY 14260
ped3@buffalo.edu

June 17, 2021

ABSTRACT

Modelling of combustion system requires modelling the underlying chemistry and the flow. Solving both systems simultaneously is computationally prohibitive. In most cases the two sub-systems have different scales and can be solved separately. The chemistry system can be solved by learning the thermochemical state of the system. It is widely known that the high dimensional thermochemical state can be expressed as a lower dimensional manifold. The lower dimensional manifold is pre-tabulated and a reverse lookup is performed while resolving the flow equations. The lower dimensional manifold is typically indexed by a small number of variables chosen by a subject matter expert and a conformal map is then used to tabulate the manifold. This strategy has no error for a reverse lookup of a nodal value (an index that is tabulated), however error creeps in for reverse lookups for non-nodal values (values that do not exist in the table). Experts agree that the standard reverse lookups for non-nodal values that rely on numerical interpolation and extrapolation techniques may completely violate the underlying physics of the system and introduce systemic errors that propagate downstream. A principled first step to reduce these non-nodal reverse lookup errors would be to validate the proposed values against the underlying physics without rerunning the whole simulation.

In this study we apply a Deep Neural Network (DNN) to learn the governing partial differential equations of the thermochemical state of 1D Steady Flame Species Conservation Equations of premixed methane/air flame using the Methane-CSM2 mechanism. The proposed DNN shows quantitatively accurate predictions for both, source species and source energy terms. This is a significant first step in creation of a framework to improve the reverse lookup accuracy. The DNN can either guide the numerical techniques or be used in conjunction with the numerical method for prediction or as a replacement for the pre-tabulated reverse lookup.

Keywords Deep learning · Combustion modeling · 1D Flamelet · Tabulated chemistry · Physics Inspired Neural Network

1 Introduction

Despite significant advances in the power and availability of computational resources and having a set of equations governing the problem, scale-resolving numerical simulations of realistic combustion systems is prohibitively expensive due to the physical complexities and multi-scale nature of the problem.

For most engineering applications, the large scale separation between the combustion chemistry(flame) and the flow allows us to make simplifying assumptions enabling increased computational efficiency [1].

Typically the combustion chemistry of a 3D flame representing the complete chemistry is approximated by an ensemble of 1D flamelets. [1, 2, 3].

Mass and Pope were one of the first to implement the manifolds to reduce the chemistry with their intrinsic low-dimensional manifolds (ILDm) [4]. Another technique to simplify the complexity of the problem is the flamelet-generated manifold (FGM) where, a multi-dimensional flame is tabulated and described as a function of mixture fraction and reaction progress variable [2, 3, 5, 6, 7].

Using the flamelet model all the chemical reactions are precomputed and mapped to a low dimensional manifold; the resulting manifold is then tabulated and looked-up at run-time. The main benefit of the flamelet model is that it allows a decoupling of the flow and the chemical reactions. The axes of the low dimensional manifold are chosen by a subject matter and are reaction progress variables that have a physical meaning and for most combustion simulations they are

Tabulating the chemistry helps an easy lookup of the flame properties as a function of mixture fraction and reaction progress variables during the flow simulations. Often the manifolds are conformally mapped from curvilinear coordinate system to a rectangular grid to store in tables. Though this technique is widely used, it has its own challenges. The manifolds are highly non-linear maps and convoluted so several values from the curvilinear coordinate system can potentially be housed non-uniquely in the same cell. And during a reverse lookup of a non-nodal (the values which have not been tabulated) a numerical interpolation technique is used. The obvious risk in using a lower dimensional manifold tabulation is clearly that it is completely removed from the underlying physics of the system it is tabulating. The higher dimensional values generated by numerical interpolation of non-uniquely indexed lower dimensional data is completely unaware of the system of governing partial differential equations.

A method to mitigate this would be to refine the tabulation i.e. discretize the lower dimensional manifold the more however the manifolds storage is expensive and querying this increased storage at run-time can significantly impact the performance of the flow simulation.

A rapid increase in data storage capabilities and a tremendous success of machine learning methods in various fields such as computer vision, robotics and health care have attracted researchers to extend this knowledge in solving physics based numerical problems [8].

Numerous methods have been developed in the recent past to use artificial neural network or deep learning to accurately predict or solve the behaviour of highly non-linear physical systems both in the higher dimensional and lower dimensional space.

Karpante *et al.* presented a hybrid framework that uses a physics based loss function in the learning objective of a neural network to ensure the predictions are scientifically consistent with the known physics of the unlabeled set. They used the output of a physics based model in combination with the physics based loss function to predict a physically consistent solution [8, 9].

Raissi *et al.* showed that using the recent advances in machine learning computation, chiefly automatic differentiation, how to differentiate neural networks with respect to their input coordinates and model parameters to obtain physics informed neural networks. Such neural networks are constrained to respect any symmetry, invariance, or conservation principles originating from the physical laws that govern the observed data, as modeled by general time-dependent and nonlinear partial differential equations [10, 11].

More recently, machine learning and neural network techniques have been applied to combustion problems including LES simulations of flames, chemistry tabulations, etc. Franke *et al.* utilized artificial neural networks in chemistry tabulation. They trained an abstract problem of an ensemble of laminar flamelets and demonstrated the application on LES-PDF simulation of Sydney flame. Self-Organising Map clustering is employed to identify clusters of data close to the chemistry composition space. A multi-layer Perceptron regression is implemented for the chemistry tabulation [12]. Lapeyre *et al.* used a previously trained CNN inside a parallel LES solver to fully resolve the subgrid-scale flame surface and comparison with DNS showed good agreement. Supervised learning was used to train the model on the DNS data and the best-trained model was frozen to execute in an LES context [13].

Some researchers like [14] have investigated the use of a DNN to completely replace the chemistry tabulation with a Neural Network in a combustion simulation using flamlets i.e. a neural network to learn the higher dimensional data as a function of the lower dimensional data. However, due to the highly non-linear and discontinuous nature of the lower dimensional manifolds the accuracy gained by a neural network is not satisfactory.

In this study, we present a deep neural network that learns the simplified 1D steady-state flame species conservation equation.

A 7 species Methane-CSM2 reduced chemistry mechanism is used [15]. An in-house numerical solver is utilized to solve for the training dataset. 1000 flames were solved with different strain rates until the flame extinguished. A physics enforced loss function is adopted to learn the differential governing equations for each of the species in the mechanism. The main objective is to predict the source production/consumption terms for each species which will further enable to predict the source energy, a very crucial parameter required in combustion simulations. Results shows a prediction accuracy of 90% for all of the species except methane, which has an accuracy of 85%. The developed model performs well for the strain-rates in the middle as against the two extremes (low strained flame and high strained just before flame extinguishes).

2 Related Work

There has been some previous work on using machine learning for combustion manifold modeling. In 2009, a thorough experimental comparison was carried out by Ihme et al. [8] using a simple Multi-Layer Perceptron (MLP) for learning a mapping function to replace the tabular lookup method and thus speed up combustion simulation calculations. They showed that a neural network approach could be more generalizable but they found it had much worse accuracy than the tabular approach. This led to the method not being adopted for combustion simulator evaluations by the community. The approach in [8] was limited to a simple range of MLP variations and focused on the optimization of the network structure relative to a particular metric. They also did not have the benefit of modern deep neural network training techniques or regularization methods and used the classical approach of sigmoid activation functions rather than rectified linear units.

3 Problem description

3.1 Reacting boundary in 1D

Conservation equations for mass, species, momentum and energy for the one-dimensional, fully compressible and viscous flame is given by:

$$\frac{\partial \rho}{\partial t} + \frac{\partial (\rho u_x)}{\partial x} = 0 \quad (1a)$$

$$\frac{\partial (\rho Y_i)}{\partial t} + \frac{\partial \rho u_x Y_i}{\partial x} = \frac{\partial}{\partial x} \left(\rho D_i \frac{\partial Y_i}{\partial x} \right) + \dot{w}_i \quad (1b)$$

$$\frac{\partial (\rho u_x)}{\partial t} + \frac{\partial (\rho u_x^2)}{\partial x} = -\frac{\partial p}{\partial x} + \frac{\partial}{\partial x} \left(\mu \frac{\partial u_x}{\partial x} \right) \quad (1c)$$

$$\frac{\partial (\rho e_t)}{\partial t} + \frac{\partial (\rho u_x H_t)}{\partial x} = \frac{\partial}{\partial x} \left(u_x \mu \frac{\partial u_x}{\partial x} \right) + \mu \frac{c_p}{Pr} \left(1 - \frac{1}{Le} \right) \frac{dT}{dx} + \frac{1}{Sc} \frac{dh}{dx} - \sum \dot{w}_i h_{f,i}^o \quad (1d)$$

where, \dot{w}_i is the mass consumption or production rate of the i^{th} species, $e_t (= e + u_x^2/2)$ is the total sensible energy, $H_t (= e_t + p/\rho)$ is the total enthalpy, and $h_{f,i}^o$ is the heat of formation of the i^{th} species. Diffusivity is assumed to be constant, Pr is the Prandtl number, Sc is the Schmidt number, Le is the Lewis number, and h is the sensible enthalpy. Prandtl (Pr) and Schmidt (Sc) numbers are both set equal to 0.70, resulting in a unity Lewis number assumption. Viscosities μ are determined from the Sutherland viscosity model, while thermal and molecular diffusivities are calculated using the definitions of Pr and Sc , respectively. Now, in 1D cartesian coordinates, the steady state solution to Eq. (1) is obtained only when the total mass flux is zero, i.e., velocity field is zero ($u_x = 0$) and Eq. (1) reduces to,

$$\frac{\partial}{\partial x} \left(\rho D_i \frac{\partial Y_i}{\partial x} \right) + \dot{w}_i = 0 \quad (2a)$$

$$\frac{\partial}{\partial x} \left(\mu \frac{c_p}{Pr} \left(1 - \frac{1}{Le} \right) \frac{\partial T}{\partial x} + \frac{1}{Sc} \frac{\partial h}{\partial x} \right) - \sum \dot{w}_i h_{f,i}^o = 0 \quad (2b)$$

Table 1: Prediction error across regression methods

Method	Error
Regression Model	
Linear regression	1.91
Linear (SGD) regression	1.99
RANSAC	4.96
Decision tree	5.10
Kernal Ridge	2.01
Kernel ridge (RBF kernel)	2.31
Bagging	4.93
Random forest	2.30
SVM (RBF kernel)	1.85
SVM (linear kernel)	2.16
SVM (polynomial kernel)	2.19

where, pressure work and viscous dissipation are neglected. The resulting system of non-linear equations are solved on discrete domain lengths (L) using a time marching technique until steady-state is reached. Dirichlet boundary conditions are used for the fuel and air side. The domain is discretized into 200 grid points in between the fuel and the air boundary and 1000 flames are solved to steady-state. Once the solution reaches steady-state the solver completes one iteration. For the next iteration flame solution is strained by a strain rate of 0.99 and the process is continued until the flame extinguishes. Each flame is then tagged with the corresponding strain rate and is called flame-key. To model the chemical kinetics reaction rates, a variety of mechanisms are adopted in the combustion community. Depending on the hydrocarbon fuel different mechanisms are chosen which closely describe the chemistry associated with the fuel of simulation. Methane is the basic hydrocarbon and one of the major products of many higher order hydrocarbons. GRI-Mech 3.0 is one of the widely used Methane mechanism to model the reaction kinetics. This mechanism consists of 53 chemical species and 325 reactions. However, in this work, Methane - CSM2 reduced mechanism is used which consists of 7 species and 4 reactions to further simplify the problem. To train the model 200,000 data points are available for a single pressure setting. The data is generated using an in-house solver which creates the flame solutions and writes the required data to an XML formatted file.

In Eq. (2b), the final term in the energy equation is represented by the total sum of the product of all the source species and their respective heat of formation and is collectively called the source energy. Source energy is one of the crucial parameters in the combustion simulation and accurate chemistry description is required to define it. In manifold mapping, the manifold is highly convoluted and is represented on a non-linear conformally mapped curvilinear coordinate systems. Given the manifold coordinates, it is difficult to lookup the source energy for non-nodal locations. Currently, the framework is built to operate on Lagrangian polynomial interpolation to lookup the manifold space and usually results in incorrect lookup resulting in simulation errors. Since the heat of formation is very high, the source energy term is in the range of 10^{10} . An incorrect lookup can thus create a very high error which is not desirable in the CFD simulations of the combustion system.

3.2 Problem setup for PINN

To determine the appropriate technique to learn the manifolds, correlation coefficient is computed in between all the dependent variables. However, no correlation is obtained between any of the parameters, making it difficult to use a classification approach. The high cost of accurate data generation through DNS and high non-linearity of the chemical kinetics involved in the combustion reactions pose a huge challenge in the process of designing a neural network. The neural network results are expected to have high prediction accuracy as the combustion reaction are highly sensitive to small changes in species and energy source terms. The prediction error defined for this study is consistent with the combustion literature and is defined as:

$$\varepsilon = \frac{2|y_{predicted} - y_{actual}|}{|y_{predicted} + y_{actual}|} \quad (3)$$

In the preliminary work of this study, numerous regression models were tested to predict the source terms. The errors for these models are listed in Table 1 where, all models yield a high prediction error. The SVM model has the least error of 1.85 amongst these models which is still not acceptable.

A fully connected deep neural network is also developed using Keras which predicted an accuracy of over 2. Running all these experiments demonstrates the complexity of the problem and it can be concluded that none of the traditional approaches can be pursued to train the network. Therefore, a physics based approach is adopted that would use the DNS data to train the DNN model and a physics based loss function that would penalize the network based on the consistency of the results by respecting the underlying physics of the problem.

This work presents a preliminary step in the manifold learning where the data-driven solution to 1D steady-state species conservation Eq. (2a) is explored as discussed in [10]. Though steady-state, the continuous time model is followed in this work to learn the equation. The non-linear partial differential equation is parametrized to obtain the general form given by:

$$u_t + \mathcal{N}[u; \lambda] = 0 \quad (4)$$

where, $u(x)$ denotes the latent solution and $\mathcal{N}[\cdot; \lambda]$ is a non-linear operator parameterized by λ [10]. In this study, since the steady-state 1D flame is considered, the time derivative term does not exist. Instead, spatial derivative is considered and the equation is parametrized accordingly. From the species conservation equation given in Eq. (2a), it is recognized only spatial derivative exists. Based on the strain rate of the flame, this equation is solved for each of the species in the Methane-CSM2 mechanism for discrete grid points until the flame reaches steady-state. Physically, straining the flame means reducing the distance between the fuel and oxidizer boundary where a counter-flow diffusion flame arrangement is considered [16, 1]. Each of the strain rate case is denoted by a flame-key which denotes the strain rate value of the flame. The corresponding flame-key and the discrete grid points then form the independent variables and ρ , \mathcal{D} , Y_i and \dot{w}_i are the parameters to be learned. The diffusion coefficient (\mathcal{D}) changes for each grid point location in the flame but remains the same irrespective of the flame-key. Now defining $f(x)$ as the left hand side of Eq. (2a) and expanding the differential term as,

$$f := \rho \left(\frac{\partial}{\partial x} \left(\mathcal{D} \frac{\partial Y_i}{\partial x} \right) \right) + \mathcal{D} \left(\frac{\partial}{\partial x} \left(\rho \frac{\partial Y_i}{\partial x} \right) \right) + \frac{\partial Y_i}{\partial x} \left(\frac{\partial}{\partial x} (\rho \mathcal{D}) \right) = -\dot{w}_i. \quad (5)$$

A physics inspired neural network is developed to learn Eq. 5. The values for ρ , \mathcal{D} and Y_i are approximated by using a deep neural network (DNN). A fully-connected network is used with 8 hidden layers and 20 nodes per each layer to train the dataset with two inputs. Hyperbolic tangent activation is used with batch gradient descent. The batch size is set to 100 data points, learning rate used is 0.001 with 10 epochs. The shared parameters between the neural networks are learned by minimizing the mean squared error loss given by:

$$MSE = MSE_u + MSE_f \quad (6)$$

where,

$$MSE_u = \frac{1}{N_u} \sum_{i=1}^{N_u} |u(x_u^i) - u^i|^2$$

and

$$MSE_f = \frac{1}{N} \sum_{i=1}^N |f(x_f^i)|^2.$$

Here, $\{x_u^i, u^i\}_{i=1}^{N_u}$ denote the training data on $u(x)$ and $\{x_f^i\}_{i=1}^{N_f}$ specify the collocation points for $f(x)$ [10, 11]. Raissi *et al.* had a time dependent differential equation in their work [10, 11]. However, in this work, since steady-state equations are used, the time dependent differential is zero. Thus, the loss functions given in [10] are modified to this specific case in which the $u(x)$ is used to denote the dependent parameters ρ , \mathcal{D} , Y_i where each of the i^{th} species is CH_4 , O_2 , CO , NO , H_2O , CO_2 , N_2 , respectively. The $f(x)$ representing the collocation points as well is modified to denote the source species terms corresponding to each of the species in the chemical kinetics mechanism. Regression through the DNN outputs the predicted dependent variables for each of the $u(x)$. The mean squared error is computed on the predicted dependent variables and the actual variables available from the training set which then corresponds to the MSE_u part of the loss function given in Eq. (6). As demonstrated by Raissi *et al.* the physics informed neural network loss $f(x)$ is obtained by solving the actual gradients in Eq. (5) which are further expanded and are given by,

$$f := 2 \left(\rho \frac{\partial \mathcal{D}}{\partial x} \frac{\partial Y_i}{\partial x} + \mathcal{D} \frac{\partial \rho}{\partial x} \frac{\partial Y_i}{\partial x} + \rho \mathcal{D} \frac{\partial^2 Y_i}{\partial x^2} \right) = -\dot{w}_i. \quad (7)$$

The problem is setup in Tensorflow environment and the gradients required in the Eq. (7) are computed using the Tensorflow gradients operator. Further details to do this are given in [10]. Solving the Eq. (7) provides the predicted

source species for each of the species in the mechanism used. Thus, the physics enforced loss function MSE_f is then the mean squared error between the predicted source species and the actual source species from the training set for each of the species. The total loss given in Eq. (6) is then optimized using the L-BFGS, a quasi-Newton, batch-gradient based optimization algorithm [17].

4 Dataset

The dataset used was generated using the Methane-CSM2 chemical kinetics mechanism. The training dataset consisted of 1000 flames at different strain rates with 200 grid points in the domain.

5 Results

Figure 1 shows the numerical solution for steady-state 1D gas-phase flame given by Eq. (2). The solutions for the temperature, gas density, methane mass fraction and source energy are shown. The fuel boundary is on the right side of the domain and the air boundary is on the left side. Both the boundaries are separated 2 *cm* apart and the normalized distance is shown on the X-axis. The Y-axis of the plots correspond to different flame-keys used to define the strain rate of the flame. The species mass fraction for each of the species vary from 0 to 1 and depending on the species reaction, their location on the plot varies either towards the fuel boundary or air boundary. In accordance with this, since the fuel used in this work is Methane (CH_4), the mass fraction of methane is 1 toward the fuel boundary on the right side and goes to 0 as it is consumed by the combustion reactions towards the air boundary as can be seen in Fig. 1c. Consequently, in case of Y_{O_2} , the mass fraction for oxygen the trend is opposite to that of Y_{CH_4} . Figure 1d shows the contour plot for source energy which is the sum of products of the source species and their respective heats of formations. It can be seen that the source energy has a very huge variability and is self-explanatory that a wrong lookup can create huge errors in the combustion simulations. Furthermore, the temperature contour plot in Fig. 1a shows the complex flame shape which is mapped on the manifolds using curvilinear coordinates.

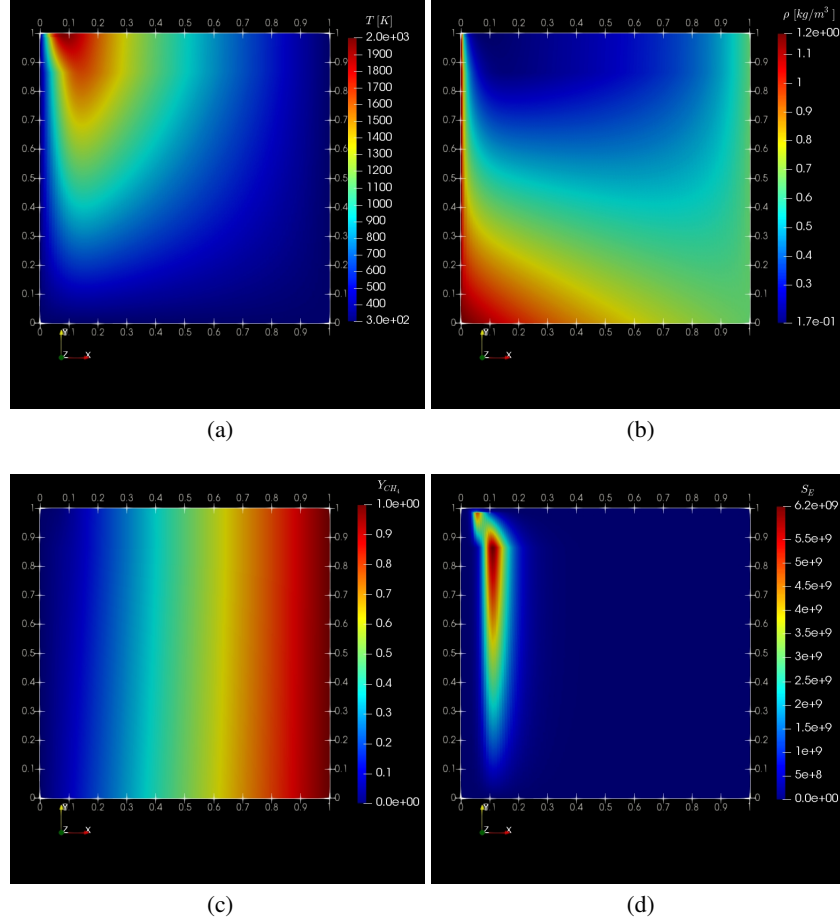


Figure 1: Steady-state 1D flame numerical solution showing (a) temperature profile, (b) density of gas-phase, (c) CH_4 mass fraction, (d) source energy.

All the data available in the solution space is used to train the network and three different flame-keys are chosen to test the network predictions. These three flame-keys correspond to the full flame, middle strain rate and strain rate corresponding to just before flame extinction. This shows the ability of the algorithm to capture the solution at the flame extremes and also at the middle solution. The initial spikes in the source energy profiles seen in the Fig.1d correspond to the source species profiles and certainly these spikes will be difficult to capture. However, the physics enforced loss function will enable the network to obtain the accurate predictions. As suggested by Bhalla *et al.* the semi-dome shape accounts for more than 50% of the input domain and shows the highest variability from flame to flame [14]. In their work, Bhalla *et al.* used four different neural networks to predict the species, heat release, temperature and source term. Furthermore, their network was designed to learn the 3D turbulent flame manifold which is represented by the reaction progress variable, mixture fraction and pressure. Their training data consisted of the flamelets for 9 different pressures and testing was conducted on 4 different pressure values. Leaky ReLU activation was used with fully connected networks. Furthermore, the network they used consists of very large number of hidden layers [14]. However, the training and testing accuracy they obtain is merely 60% and 55%, respectively, for temperature. This accuracy is certainly low and can create significant issues in the combustion simulation results. Furthermore, their prediction model does not perform well with the heat release. Considering the complexity of the manifolds and the large range of source term variation provides an explanation for the poor performance of their model.

Thus in the present work, instead of directly learning the manifold, a simple problem of learning the governing steady-state flame equations is chosen. With the hyperbolic tangent activation the network is able to predict the source species with accuracy above 90%. However, with this activation the network does not predict accurate values for ρ and Y_i . When the activation is changed to ReLU instead, the network predicts ρ and Y_i with accuracy greater than 95%. However, in that case the source species term prediction becomes less accurate. It is unknown why this phenomena is

observed and more work is required to explain it better. Nevertheless, the main objective of this work is to predict the source species terms accurately so they can be further utilized to predict the source energy.

Figure 2 shows the source predictions for CH_4 for three different flame-keys representing the full flame, medium strain rate flame and just before extinguishing. The flame-key for each case is shown in the title of each plot and corresponds to the strain-rate for that flame, respectively. The accuracy of prediction is about 85% for this case. More experiments and hyperparameter tuning did not provide any insights as to how to improve the results. Nevertheless, it can be seen that the network predicts accurate shape of the source profile.

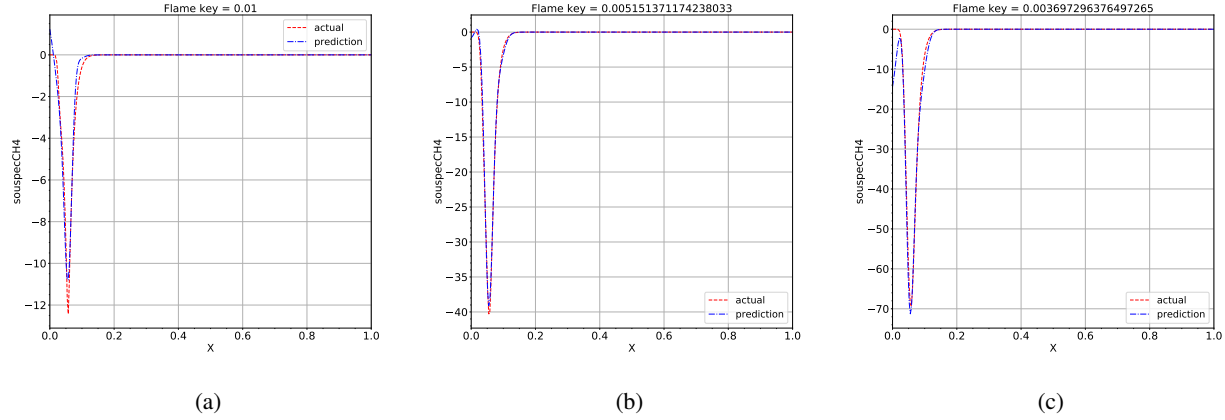


Figure 2: Source species term for CH_4 for (a) full flame, (b) medium strain rate, (c) flame just before extinguished.

Figures 3 to 6 shows the actual and predicted source species comparison for O_2 , CO_2 , H_2O and CO . Similar to Fig. 2, three different plots are shown corresponding to three different strain-rates. It can be seen from the plots that the prediction for all the species for all three strain-rates is significantly better than that for CH_4 . For the full flame and just before extinguishing the flame, the network predicts the source terms less accurately as compared to the medium strain-rate case. Increasing the number of layers and hyperparameter tuning did not perform better than the shown results. Nevertheless, the prediction accuracy obtained for all the species is above 92%. It is interesting to note that the neural network is able to capture the spikes in the data accurately. For the CO source, as shown in Fig. 6, there are two spikes and the network is able to capture both the spikes accurately.

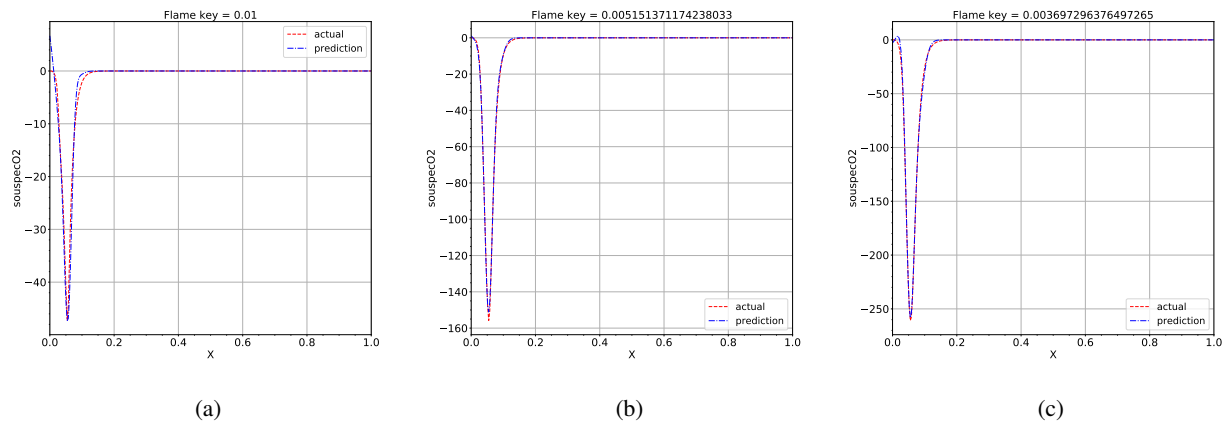
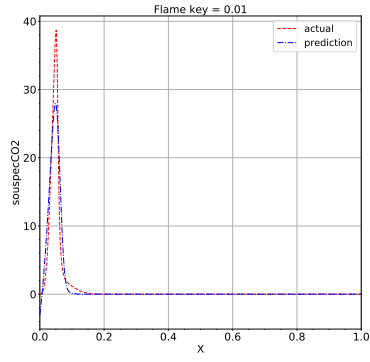
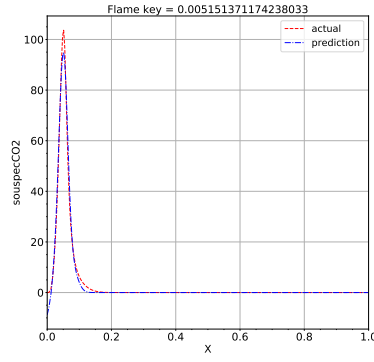


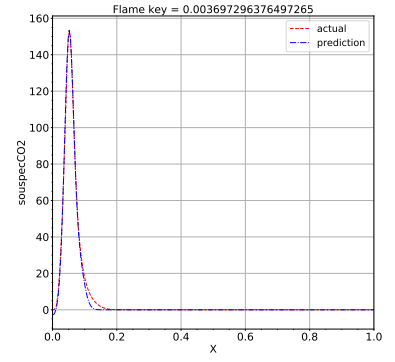
Figure 3: Source species term for O_2 for (a) full flame, (b) medium strain rate, (c) flame just before extinguished.



(a)

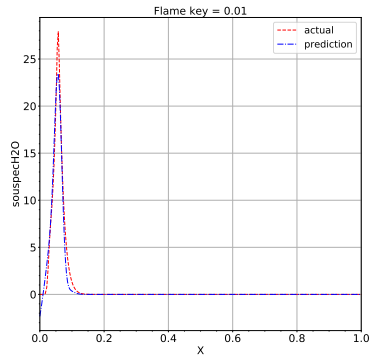


(b)

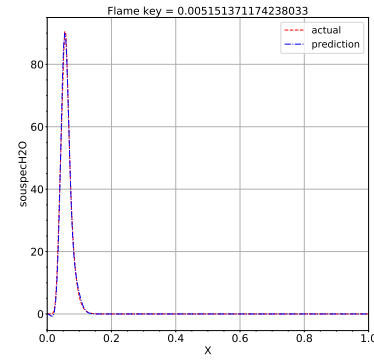


(c)

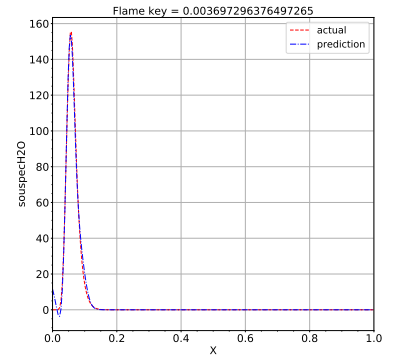
Figure 4: Source species term for CO_2 for (a) full flame, (b) medium strain rate, (c) flame just before extinguished.



(a)



(b)



(c)

Figure 5: Source species term for H_2O for (a) full flame, (b) medium strain rate, (c) flame just before extinguished.

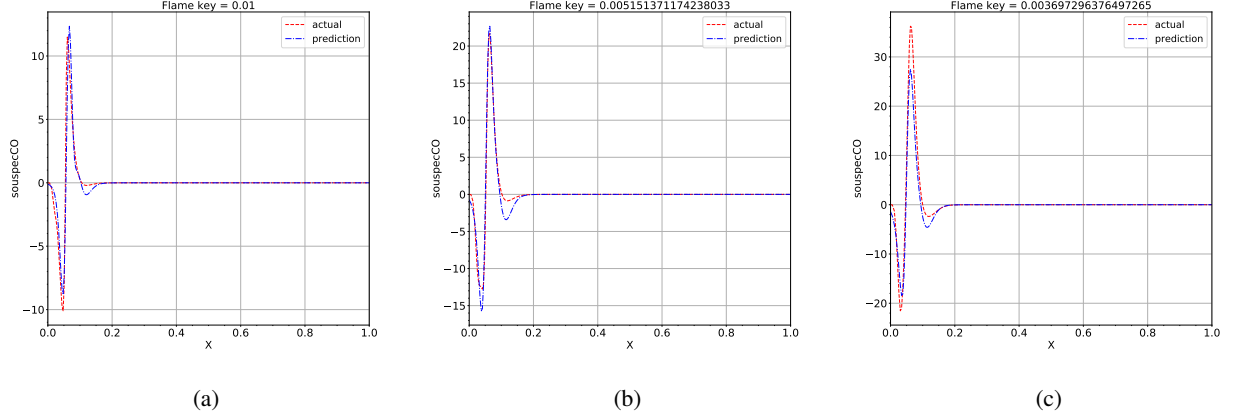


Figure 6: Source species term for CO for (a) full flame, (b) medium strain rate, (c) flame just before extinguished.

Figure 7 shows the for the actual and predicted source energy. Using the source species predictions obtained for each of the flame key, source energy can be computed by knowing the heat of formations of each of the species at 298 K . Table 2 provides the list of heat of formation in $kJ/kmol$ for all the species in the Methane-CSM2 mechanism. Knowing the source species and corresponding heat of formation, the source energy is the sum of product of both as shown in Eq. (2b). For each flame-key, source energy can then be computed and compared to the numerically computed values using CFD. As shown in Fig. 7, the source energy prediction is very accurate for all the three flame keys or strain rates discussed. At strain rate with flame-key 0.01 the prediction has an error of 20% which corresponds to the error due to CH_4 source species prediction. However, for the later flame keys the prediction is within $\pm 3\%$ of the actual value. Considering that the energy equation is not learnt in this study, the source energy predicted by the neural network is highly accurate and certainly can be used to tabulate the flamelets and weight the errors on the manifolds.

Table 2: Heat of formations for each species

Species	$h_{f,i}^o [kJ/kmol]$
CH_4	-74,831
CO	-110,541
CO_2	-393,546
H_2O	-241,845
N_2	0
NO	90,297
O_2	0

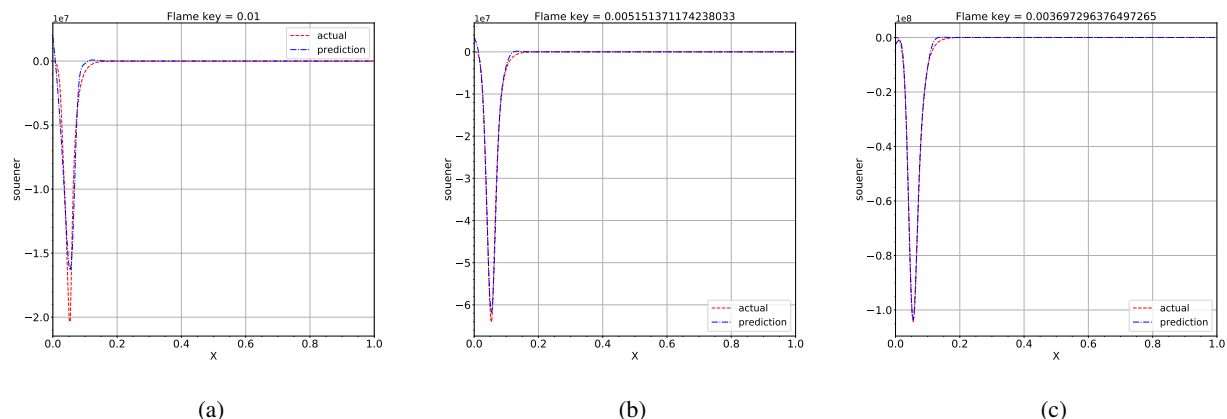


Figure 7: Source energy for (a) full flame, (b) medium strain rate, (c) flame just before extinguished.

The reduced chemical kinetics mechanism has shown encouraging results in the data-driven solution to the 1D steady-state species conservation equations. Without learning the energy equation, the prediction of source energy is highly accurate. However, to predict the temperature of the flamelets, it is essential to learn the 1D energy equation. With this study it is expected that the current data-driven solutions can be further extended to learn the 3D manifolds that are expressed in the form of mixture fraction, reaction progress variable and the variance of mixture fraction. Furthermore, the network seems to learn for a reduced mechanism but, it is not tested on GRI-Mech 3.0 which has 53 species and significantly more reactions. The logical next step to test the network capabilities is to implement the data-driven solution to the flamelet equations for a GRI-Mech 3.0 environment and check the capabilities of the data-driven solution on all the 53 species and 322 reactions. Furthermore, it is essential to train the network on the temperature data and provide a data-driven solution to the 1D energy equation. These are the essential future prospects to learn the manifolds so it can be used in the flow simulations. Nevertheless, the results discussed here demonstrate the capabilities of the data-driven solution to learn steady-state flamelet equations.

6 Conclusion

We have shown how a neural network can be trained to learn the steady state 1D flame equation. This construction enables tackling a wide range of problems in computational science and introduces a potentially disruptive technology leading to the development of new data-efficient and physics-informed learning machines, new classes of numerical solvers for partial differential equations, as well as new data-driven approaches for model inversion and systems identification.

Physics Informed Neural Networks provide a new approach of modelling complex flow kinetics while respecting the underlying laws of physics described by general nonlinear partial differential equations. The DNN implemented in this study provides fairly accurate estimation of source species and consequently source energy terms in 1D flame equations and confirms the potentials of implementing physics informed neural network to highly non linear chemical kinetics.

The DNN was trained to learn the 1D steady-state species conservation equation using the strain rate, density and distance. The DNN predicts species mass fractions, source species and source energy for each strain rate.

Prediction results show an accuracy of about 90% for all the species. The predicted source energy is highly accurate with an error within $\pm 3\%$.

7 Future Work

Future work will focus on learning the 1D energy equation to predict the temperature and extend the network to learn the equations of a mechanism that has significantly more species like GRI-Mech 3.0.

Future work will also focus on building a improved reverse lookup framework that leverages the DNN presented in this work either as a Validator or as a Predictor.

References

- [1] Norbert Peters. Turbulent combustion, 2001.
- [2] JA Van Oijen and LPH De Goey. Modelling of premixed laminar flames using flamelet-generated manifolds. *Combustion Science and Technology*, 161(1):113–137, 2000.
- [3] JA Van Oijen, FA Lammers, and LPH De Goey. Modeling of complex premixed burner systems by using flamelet-generated manifolds. *Combustion and Flame*, 127(3):2124–2134, 2001.
- [4] Ulrich Maas and Stephen B Pope. Implementation of simplified chemical kinetics based on intrinsic low-dimensional manifolds. In *Symposium (International) on Combustion*, volume 24, pages 103–112. Elsevier, 1992.
- [5] Charles D Pierce and Parviz Moin. Progress-variable approach for large-eddy simulation of non-premixed turbulent combustion. *Journal of fluid Mechanics*, 504:73–97, 2004.
- [6] Charles David Pierce and Parviz Moin. *Progress-variable approach for large-eddy simulation of turbulent combustion*. stanford university California, USA, 2001.
- [7] Brian T Bojko and Paul E DesJardin. Formulation and assessment of flamelet-generated manifolds for reacting interfaces. *Combustion and Flame*, 173:296–306, 2016.
- [8] Anuj Karpatne, Gowtham Atluri, James H Faghmous, Michael Steinbach, Arindam Banerjee, Auroop Ganguly, Shashi Shekhar, Nagiza Samatova, and Vipin Kumar. Theory-guided data science: A new paradigm for scientific discovery from data. *IEEE Transactions on Knowledge and Data Engineering*, 29(10):2318–2331, 2017.
- [9] Anuj Karpatne, William Watkins, Jordan Read, and Vipin Kumar. Physics-guided neural networks (pgnn): An application in lake temperature modeling. *arXiv preprint arXiv:1710.11431*, 2017.
- [10] Maziar Raissi, Paris Perdikaris, and George Em Karniadakis. Physics informed deep learning (part i): Data-driven solutions of nonlinear partial differential equations. *arXiv preprint arXiv:1711.10561*, 2017.
- [11] Maziar Raissi, Paris Perdikaris, and George Em Karniadakis. Physics informed deep learning (part ii): Data-driven discovery of nonlinear partial differential equations. *arXiv preprint arXiv:1711.10566*, 2017.
- [12] Lucas LC Franke, Athanasios K Chatzopoulos, and Stelios Rigopoulos. Tabulation of combustion chemistry via artificial neural networks (anns): Methodology and application to les-pdf simulation of sydney flame I. *Combustion and Flame*, 185:245–260, 2017.
- [13] CJ Lapeyre, A Misdariis, N Cazard, and T Poinso. A-posteriori evaluation of a deep convolutional neural network approach to subgrid-scale flame surface estimation. 2018.
- [14] Sushrut Bhalla, Matthew Yao, Jean-Pierre Hickey, and Mark Crowley. Compact representation of a multi-dimensional combustion manifold using deep neural networks. In *European Conference on Machine Learning*, 2019.
- [15] J Bibrzycki and T Poinso. Reduced chemical kinetic mechanisms for methane combustion in o₂/n₂ and o₂/co₂ atmosphere. *Working note ECCOMET WN/CFD/10*, 17, 2010.
- [16] R Stephen. Turns. an introduction to combustion: concepts and applications. *Mechanical Engineering Series. McGraw Hill*, 2000.
- [17] Dong C Liu and Jorge Nocedal. On the limited memory bfgs method for large scale optimization. *Mathematical programming*, 45(1-3):503–528, 1989.